

Fat-distribution patterns and future type-2 diabetes

Running head: Fat distribution and diabetes

Hajime Yamazaki, MD, PhD¹, Shinichi Tauchi, RT², Jürgen Machann PhD^{3,4,5}, Tobias Haueise^{3,4,5},
Yosuke Yamamoto MD, PhD⁶, Mitsuru Dohke, MD⁷, Nagisa Hanawa, MD⁷, Yoshihisa Kodama,
MD, PhD⁸, Akio Katanuma, MD, PhD⁹, Norbert Stefan MD^{4,5,10}, Andreas Fritsche MD^{4,5,10}, Andreas
L. Birkenfeld MD^{4,5,10}, Róbert Wagner, MD^{4,5,10,11,12*}, Martin Heni, MD^{4,5,10,13,14*}

* Róbert Wagner and Martin Heni contributed equally.

1) Section of Clinical Epidemiology, Department of Community Medicine, Graduate School of
Medicine, Kyoto University, Kyoto, Japan

2) Department of Radiology, Keijinkai Maruyama Clinic, Sapporo, Japan

3) Department of Radiology, Section on Experimental Radiology, Eberhard-Karls University,
Tübingen, Germany

4) German Center for Diabetes Research (DZD), Neuherberg, Germany

5) Institute for Diabetes Research and Metabolic Diseases of the Helmholtz Center Munich at the
University of Tübingen, Tübingen, Germany

6) Department of Healthcare Epidemiology, School of Public Health in the Graduate School of

Medicine, Kyoto University, Kyoto, Japan

7) Department of Health Checkup and Promotion, Keijinkai Maruyama Clinic, Sapporo, Japan

8) Department of Radiology, Teine Keijinkai Hospital, Sapporo, Japan

9) Center for Gastroenterology, Teine Keijinkai Hospital, Sapporo, Japan

10) Department of Internal Medicine, Division of Diabetology, Endocrinology and Nephrology,
Eberhard-Karls University, Tübingen, Germany

11) German Diabetes Center (Deutsches Diabetes-Zentrum/DDZ), Leibniz Center for Diabetes
Research at Heinrich-Heine-University Düsseldorf, Düsseldorf, Germany

12) Department of Endocrinology and Diabetology, University Hospital Düsseldorf, Heinrich-Heine-
University Düsseldorf, Düsseldorf, Germany

13) Institute for Clinical Chemistry and Pathobiochemistry, Department for Diagnostic Laboratory
Medicine, University Hospital Tübingen, Tübingen, Germany

14) Department of Internal Medicine I, University of Ulm, Ulm, Germany

Correspondence: Hajime Yamazaki, MD, PhD

Section of Clinical Epidemiology, Department of Community Medicine, Graduate School of
Medicine, Kyoto University

54 Kawahara-cho, Syogoin, Sakyo-ku, Kyoto 606-8507, Japan

Phone: +81-75-366-7655

Fax: +81-75-366-7655

E-mail: yamazaki-myz@umin.ac.jp

Word count (text only): 3995

Number of tables and figures: 3 tables and 1 figure

Abstract

Fat accumulation in the liver, pancreas, skeletal muscle, and visceral bed relates to type-2 diabetes (T2D). However, the distribution of fat among these compartments is heterogenous and it is unclear whether specific distribution patterns indicate high T2D risk. We therefore investigated fat-distribution patterns and their link to future T2D. From 2168 individuals without diabetes who underwent computed tomography in Japan, this case-cohort study included 658 randomly selected individuals and 146 incident cases of T2D over 6 years of follow-up. Using data-driven analysis (k-means) based on fat content in the liver, pancreas, muscle, and visceral bed, we identified four fat-distribution clusters: Hepatic steatosis, Pancreatic steatosis, Trunk myosteosis, and Steatopenia. Compared with the Steatopenia cluster, the adjusted hazard ratios (95% CIs) for incident T2D were 4.02 (2.27-7.12) for the Hepatic steatosis cluster, 3.38 (1.65-6.91) for the Pancreatic steatosis cluster, and 1.95 (1.07-3.54) for the Trunk myosteosis cluster. The clusters were replicated in 319 German individuals without diabetes who underwent magnetic resonance imaging and metabolic phenotyping. The distribution of AUC-glucose across the four clusters found in Germany was similar to the distribution of T2D risk across the four clusters in Japan. Insulin sensitivity and insulin secretion differed across the four clusters. Thus, we identified patterns of fat distribution with different T2D risks presumably due to differences in insulin sensitivity and insulin secretion.

Main text

The incidence of type-2 diabetes (T2D) is increasing, and more individualized approaches to preventing and treating T2D are needed (1). Obesity is the main modifiable risk factor for T2D. The classification of obesity is typically based on body mass index (BMI). Although BMI is an easy-to-determine indicator of overall adiposity, it gives no information about the location of accumulated fat. This is important as the location of fat storage appears to be crucial for T2D risk (2).

Fat accumulation in the visceral bed (2; 3), liver (4-6), pancreas (7; 8), and skeletal muscle (9; 10) is associated with T2D. “Visceral fat” refers to accumulation of adipose tissue in the peritoneum and retroperitoneum (11). Having large amounts of visceral fat is strongly linked to whole-body insulin resistance, which is an important predictor of T2D risk (3; 11). Further important locations for excessive lipid accumulation include the liver (in hepatocytes), pancreas (in adipocytes), and skeletal muscle (intramyocellular and in adipocytes). Proposed mechanisms connecting increased lipid deposition in these three organs with T2D include hepatic insulin resistance (12; 13), impairment of pancreatic insulin secretion (8; 14), and muscle insulin resistance (9; 15), respectively. The development of T2D probably depends on a complex interplay of those three mechanisms (13; 14). Indeed, our previous longitudinal study showed how T2D risk is related to an interaction between obesity and pancreas fat (7), for which there is also histological and genetic evidence (16; 17). While it has been proposed that some individuals have distinct patterns of body-fat distribution that determine their likelihood to develop T2D (7; 10; 18), the approaches that led to

those proposals were often hypothesis-driven and focused on effects of a limited number of fat compartments.

To identify previously undetected patterns of fat storage, we did a case-cohort study in Japan, using data-driven cluster analysis to partition participants based on the distribution of liver, pancreas, muscle, and visceral fat measured by computed tomography (CT). We then studied the longitudinal association of membership in the resulting clusters with incident T2D. Then, cluster validation was done in Germany, among people with an increased risk of T2D. In that study, body fat was quantified by magnetic resonance imaging (MRI) and proton magnetic resonance spectroscopy ($^1\text{H-MRS}$), and additional glycemic traits were assessed through 75 g oral glucose tolerance tests (OGTT).

Research Design and Methods

Design

We conducted a retrospective case-cohort study in Japan and a cross-sectional study in Germany. Case-cohort studies use data from individuals who are randomly selected members (i.e. subcohort) of a “total” cohort, and they additionally use data on all of the cases in which the outcome of interest occurred. This leads to efficient sampling by reducing the need to perform expensive measurements in a large sample of controls, while still using information on all cases, even if the outcome is not

frequent (19). The benefit of the case-cohort design over a case-control design is that the randomly selected subcohort can be used to estimate characteristics of the total cohort and to select controls for multiple outcomes (20). The study flow diagram with an explanation of the methods is in

Supplementary Figure 1.

Participants in Japan

We used secondary data collected during health examinations with CT at Keijinkai Maruyama Clinic, Sapporo, Japan. CT equipment is easily accessible in Japan (21). We examined data from 2793 individuals who underwent health examinations including baseline CT between May 1, 2008 and March 31, 2013. We excluded all individuals with diabetes mellitus at baseline ($n = 216$), as well as those who met CT-exclusion criteria ($n = 27$), those whose BMI data were missing ($n = 1$), and those without follow-up data ($n = 381$). A radiologist, who was blinded to data other than CT images, excluded individuals with baseline CT scans that had substantial artifacts, as well as those with pancreatic calcification, space-occupying lesions in the pancreas, ambiguous pancreatic margin, pancreatic atrophy, splenic resection, or pancreatic resection. From the original 2793 individuals, 2168 were eligible for this study (i.e., the “total” cohort). During the median follow-up period of 6.27 (interquartile range [IQR]: 4.04-8.20) years, there were 146 incident cases of T2D in the total cohort. From the viewpoint of relative efficiency (22), a 1:4 ratio of case to control was favorable for this case-cohort study. We randomly selected 30% of the total cohort, and that 30% (658 participants)

thus became the subcohort. After pooling this randomly selected subcohort and all remaining incident T2D cases who were not selected in this subcohort, we obtained a 1:4 ratio of cases (n = 146) to non-cases (n = 608). There were 50 participants who had an incident case of T2D and were also in the randomly selected subcohort. Altogether, this case-cohort study comprised 754 participants.

Participants in Germany

We used secondary data from the Tübingen Diabetes Family Study (TDFS) (23). This study recruited individuals with at least one of the following: known prediabetes, family history of diabetes, history of gestational diabetes, or obesity. We included individuals who underwent MRI/¹H-MRS to quantify visceral fat (T1-weighted fast spin echo), liver fat (¹H-MRS), pancreas fat, and muscle fat (3D multiecho chemical-shift encoding-based abdominal MRI), enabling assessment of all fat compartments corresponding to the CT study.

Measurement of indices of fat distribution in Japan

We quantified four fat-distribution indices on unenhanced CT: liver attenuation (liver fat), pancreas attenuation (pancreas fat), muscle attenuation (fat in trunk muscle), and visceral fat area (visceral fat). We also measured muscle area. Unenhanced CT images in which each slice was 10 mm thick were obtained using a single helical scanner (Asteion/KG TSX-021B, Toshiba, Otawara, Japan) and

a multislice helical scanner (Alexion TSX-032A; Toshiba, Otawara, Japan) before and after May 2012, respectively.

Using a workstation (TWS-5000, Toshiba, Otawara, Japan), and under the supervision of a radiologist, seven radiologic technologists who were blinded to data other than CT images measured liver attenuation and pancreas attenuation. Lower liver attenuation (Hounsfield units [HU]) indicated greater hepatic steatosis (24). Three round regions of interest (ROIs) with areas of 1.0 cm² were positioned on the hepatic anterior segment, posterior segment, and left lobe. The mean attenuation of those three ROIs was used to derive liver fat content. Our previous study regarding inter-rater reliability of this measure demonstrated an excellent intraclass correlation coefficient (95% confidence intervals [95% CI]) of 0.98 (0.96-0.99) (7). Similarly, pancreas fat was measured by analyzing pancreas attenuation on CT images. This measure also negatively correlates with pancreas fat (25). Three ROIs with areas of 1.0 cm² were positioned on thick segments of the pancreatic head, body, and tail, to minimize partial-volume effects. The mean pancreas attenuation from these three ROIs was used as the index of pancreatic steatosis. Our previous study regarding inter-rater reliability showed an intraclass correlation coefficient (95% CI) of 0.89 (0.82-0.94) (7).

Using an Automated Body composition Analyzer using Computed tomography image Segmentation (ABACS) software (Voronoi Health Analytics Inc., Vancouver, Canada) and sliceOmatic software (Tomovision, Magog, Canada), an experienced radiologic technologist who was blinded to participants information measured muscle area, muscle attenuation, and visceral fat

area at the level of the L3 lumbar segment. Previous studies showed that L3-level measurements of muscle area and visceral fat area had the highest correlation with whole-body muscle and whole-body visceral fat (26). The ABACS software automatically recognizes these tissues based on CT attenuation thresholds (27). Muscle attenuation was automatically calculated as mean attenuation of muscle area. Lower muscle attenuation indicates more muscle fat (28; 29). We evaluated intra-rater reliability in 50 randomly selected participants: intraclass correlation coefficients of muscle area, muscle attenuation, and visceral fat area were all 1.00.

Measurement of indices of fat distribution in Germany

All magnetic resonance (MR) examinations were performed, using a 3T whole-body imager (Magnetom Vida, Siemens Healthineers, Erlangen, Germany). Visceral fat volume, pancreas fat, and muscle fat were measured by MRI, and liver fat was quantified by ^1H -MRS. Additionally, muscle area was measured. Volumetric quantification of visceral fat was performed from T1-weighted fast-spin echo images with a slice thickness of 10 mm acquired between the hip and the thoracic diaphragm (30) applying an automatic fuzzy c-means algorithm and orthonormal snakes (31). To determine proton density fat fraction (PDFF) in pancreas and muscle, a 3D multi-echo gradient-echo chemical shift encoding-based technique was applied, recording 6 images with different echo times and a slice thickness of 3 mm in a single breath-hold (32). Pancreas fat was quantified by manually drawing 3 regions of interest in the head, body, and tail of the pancreas. ^1H -MRS of the liver was

done applying a single voxel STEAM technique in a volume of interest of $3 \times 3 \times 2 \text{ cm}^3$ in the posterior part of segment VII (30). Signals of methylene and methyl protons (fat) were referenced to the sum of the fat and water signals to calculate liver fat in percent. All evaluations were performed by an experienced medical physicist on a standalone PC using Matlab R2014A (The MathWorks Inc., Natick, Mass) for visceral fat and liver fat measurement and on the workstation of the imager for pancreas fat measurement. Muscle fat and muscle area were assessed at the level of the L3 lumbar segment. For this purpose, a random sample of 50 manually segmented PDFF MR images at the level of the L3 lumbar segment were used to train an ensemble of five 2D U-Net models (nnU-Net) (33) using five-fold cross-validation to perform the segmentation of muscle PDFF on a cluster GPU (Tesla V100, NVIDIA, Santa Clara/CA, USA). The nnU-Net ensemble showed a mean Dice similarity coefficient (95% CI) of 0.9725 (0.9705-0.9744). The mean PDFF and MR image pixel dimensionality were used to derive the muscle fat and muscle area from the automatically segmented muscles, respectively (**Supplementary Figure 2**).

Assessment of T2D incidence in Japan

The presence of at least one of the following criteria was used to diagnose T2D: fasting plasma glucose $\geq 126 \text{ mg/dL}$, HbA1c $\geq 6.5\%$ (48 mmol/mol), or having a prescription for any anti-diabetes medication. The incidence of T2D was evaluated from the day of the baseline health examination with CT imaging to the day of the last health examination before December 31, 2018.

Assessment of glycemic traits and aerobic capacity in Germany

After an overnight fast, a five-point 75 g OGTT was performed. Glycemia was evaluated using the area-under-the-curve (AUC) of glucose from 0 to 120 minutes (AUC Glucose₀₋₁₂₀). Insulin sensitivity was assessed by the non-esterified fatty acids-based insulin sensitivity index (NEFA-ISI), and insulin secretion was quantified by the ratio of the AUC of C-peptide from 0 to 30 minutes to the AUC of glucose from 0 to 30 minutes (AUC C-peptide₀₋₃₀/AUC Glucose₀₋₃₀) (34). To estimate insulin secretion adjusted for insulin sensitivity, we computed the residuals of AUC C-peptide₀₋₃₀/AUC Glucose₀₋₃₀ from a linear regression of this variable on NEFA-ISI and its quadratic term. Analytes were measured as described previously (23). We evaluated aerobic capacity (maximal oxygen uptake, VO₂ max) on a bicycle ergometer, as described previously (35).

Cluster analysis

To identify fat-distribution clusters in Japan, we used liver attenuation, pancreas attenuation, muscle attenuation, and visceral fat area. Liver attenuation, pancreas attenuation, and muscle attenuation were “flipped,” such that higher values corresponded to more fat. To account for sex-related differences in fat distribution, each of the four indices was standardized (mean = 0, standard deviation [SD] = 1) separately for the men and for the women in the randomly selected subcohort (n = 658). With these sex-stratified standardized variables, we conducted k-means clustering using the

kmeans function in R. We selected a k value of 4 based on visual inspection of the elbow plot and majority vote of multiple indices to determine the best number of clusters using the Nbclust function in R (36). We created a two-dimensional cluster plot based on principal components analysis using the fviz_cluster function in R. Jaccard similarities to the original cluster with 2000 re-samplings were calculated to evaluate cluster stability using the cboot.hclust function in R. We named the clusters based on cluster variable means.

To assign each of the 754 Japanese participants to one of the clusters generated from the randomly selected subcohort, we used the cluster centroids to identify the cluster nearest to each participant by performing k-nearest neighbor classification with $k = 1$ using the knn function in R. We used the assigned clusters to evaluate the risk of T2D.

As a validation test of the fat-distribution clusters, we applied the cluster analysis described above to 319 participants in the TDFS German cohort. We used the validated clusters to evaluate glycemic traits in the cohort in Germany.

Statistical analysis

Baseline characteristics of the participants were compared between fat-distribution clusters using Fisher's exact test for categorical data and Wilcoxon's rank-sum tests or the Kruskal-Wallis test for continuous data.

Using the data from Japan, we conducted weighted Cox regression analyses to evaluate the

association between the fat-distribution clusters and the incidence of T2D. Besides unadjusted analysis and analyses adjusted for age and sex, we conducted three multivariable analyses. In model 1, we adjusted for age, sex, alcohol intake (daily alcohol intake or not), current smoking, and muscle area. In model 2, we further adjusted for BMI. In model 3, we further adjusted for systolic blood pressure, diastolic blood pressure, triglycerides, HDL-cholesterol, LDL-cholesterol, antihypertensive drugs, and lipid-lowering drugs. Despite a high correlation of BMI with visceral fat, we adjusted for BMI to investigate the importance of fat distribution clusters independent from BMI. We also quantified interactions among pairs of the four fat indices (liver attenuation, pancreas attenuation, muscle attenuation, and visceral fat area on CT) regarding the incidence of T2D.

Using the data from Germany, we estimated the mean and 95% CI of the AUC Glucose₀₋₁₂₀, NEFA-ISI, AUC C-peptide₀₋₃₀/AUC Glucose₀₋₃₀, and AUC C-peptide₀₋₃₀/AUC Glucose₀₋₃₀ residuals in the fat-distribution clusters. We also compared these glycemic traits using Wilcoxon's rank-sum test. We also quantified interactions among pairs of the four fat indices (liver fat, pancreas fat, muscle fat, and visceral fat volume on MRI) regarding the AUC Glucose₀₋₁₂₀. In addition, linear regression models were used to evaluate the association of each fat index with NEFA-ISI, AUC C-peptide₀₋₃₀/AUC Glucose₀₋₃₀, AUC C-peptide₀₋₃₀/AUC Glucose₀₋₃₀ residuals, and VO2 max.

For statistical analyses, R version 4.0.5 (R Foundation for Statistical Computing, Vienna, Austria) and Stata 17 (StataCorp, College Station, TX, USA) were used.

Ethical considerations

The study in Japan was approved by the ethics committees of Kyoto University and Keijinkai Maruyama Clinic, and written informed consent was not required because it was retrospective. The study in Germany was approved by the ethics committee of the University of Tübingen, and written informed consent was provided by all participants before enrollment.

Data and resource availability

The data generated during the current study are not publicly available due to them containing information that could compromise research participant privacy/consent. No applicable resources were generated or analyzed during the current study.

Results

Participants' characteristics and K-means clustering

Table 1 shows baseline data. K-means clustering identified four similarly configured clusters in both Japan and Germany (**Figure 1** and **Supplementary Figure 3**). Participants in Cluster 1 had the highest levels of liver fat as well as somewhat high levels of visceral fat, so Cluster 1 was called the Hepatic steatosis cluster. Participants in Cluster 2 had the highest levels of pancreas fat, as well as somewhat high levels of visceral fat and muscle fat, so Cluster 2 was called the Pancreatic steatosis

cluster. Participants in Cluster 3 had high levels of muscle fat, so Cluster 3 was called the Trunk myosteator cluster. Participants in Cluster 4 had low levels of fat in all compartments, so Cluster 4 was called the Steatopenia cluster. Details of the clusters are shown in **Supplementary table 1** and **Supplementary table 2**. The stability of each cluster was estimated as its Jaccard mean, which was equal to or greater than 0.8 for all clusters except Cluster 2 in Germany, for which it was 0.64.

Association between fat-distribution clusters and the incidence of T2D

With the Steatopenia cluster as the reference, hazard ratios (HRs) and confidence intervals (95% CIs) for the association of the other three clusters with the incidence of T2D are shown in **Table 2**. In the unadjusted analysis, HRs for T2D incidence in all three clusters were greater than the reference value of 1. After adjustment for age, sex, alcohol intake, current smoking, and muscle area, the associations of steator with T2D were still substantial for all three clusters. After further adjustment for BMI, the effect sizes were smaller, but the HRs for T2D incidence in both the Hepatic steator cluster and the Pancreatic steator cluster were still greater than the reference value of 1 ($p < 0.001$ and $p = 0.016$, respectively). Results of pairwise comparisons are shown in **Supplementary table 3**.

Pairwise interactions of fat compartments regarding T2D risk

Three interactions were found (**Supplementary table 4**), and all three involved pancreas fat: visceral fat and pancreas fat (P for interaction = 0.004), liver fat and pancreas fat (P for interaction = 0.055),

and muscle fat and pancreas fat (P for interaction = 0.001).

Differences in glycemic traits across fat-distribution clusters

With the Steatopenia cluster as the reference, glycemic traits of the other three fat-distribution clusters are shown in **Table 3**. Participants who were in the Hepatic steatosis cluster had the highest glycemia (P < 0.001) and the lowest insulin sensitivity (P < 0.001). Compared with the participants in the Steatopenia cluster, those in the Pancreatic steatosis cluster had higher glycemia (P < 0.001), lower insulin sensitivity (P < 0.001), and the lowest insulin secretion adjusted for insulin sensitivity (P = 0.081). Among those in the Trunk myosteatorosis cluster, glycemia was high (P < 0.001), insulin sensitivity was low (P < 0.001), and insulin secretion adjusted for insulin sensitivity was low (P = 0.081). Results of pairwise comparisons are shown in **Supplementary table 5**.

Pairwise interactions of fat compartments regarding glycemia

Five interactions were found (**Supplementary table 6**). P values for all five interactions were < 0.01.

The only interaction term that was not significantly different from zero was the term for the interaction between liver fat and muscle fat (P for interaction = 0.34).

Association of single fat compartments with insulin and with aerobic capacity

All four fat compartments were associated with insulin sensitivity (**Supplementary table 7**, P <

0.001), with the largest effect size observed for visceral fat. Only pancreas fat was associated with lower insulin secretion adjusted for insulin sensitivity ($P = 0.016$). All four fat compartments were associated with lower aerobic capacity, with the largest effect size observed for muscle fat.

Discussion

Individuals without diabetes had a highly heterogeneous distribution of fat in the liver, pancreas, skeletal muscle, and visceral areas. Independently applying data-driven partitioning procedures to two cohorts, we identified four patterns (four clusters) of fat distribution: a Hepatic steatosis cluster, a Pancreatic steatosis cluster, a Trunk myosteatosis cluster, and a Steatopenia cluster. An individual's risk of T2D was associated with a specific pattern of fat distribution. Compared with the individuals who had low levels of fat in all areas studied (i.e., those in the Steatopenia cluster), those in the other three clusters were at a greater risk of incident T2D. The distribution of T2D risk among clusters in one cohort was similar to the distribution of glycemia among clusters in the other cohort. Insulin sensitivity and insulin secretion differed across clusters, which indicates the pathophysiologic contributions of each fat-distribution pattern to T2D risk (**Supplementary figure 4**).

Our results are consistent with those of previous studies: individuals with high amount of visceral fat and liver fat had a high risk of T2D. Both visceral fat at baseline and its increase over time were strongly linked to a high incidence of T2D (3). In a meta-analysis, liver fat was found to be associated with a twofold higher risk of T2D (12). The underlying mechanism most likely

involves hepatic and whole-body insulin resistance, either by direct effects on hepatocytes and/or by effects on remote organs mediated by hepatokines (37; 38). Our present study confirmed the well-established associations of visceral fat and liver fat with insulin resistance.

Two longitudinal studies detected associations of pancreas fat accumulation with increased risk of T2D (7; 18). The underlying mechanism is thought to be unfavorable effects of this local fat accumulation on pancreatic insulin secretion (8; 14). However, pancreas fat is not always detrimental for insulin secretion. In previous MRI and pathological studies, the association between pancreas fat and insulin secretion impairment was found in individuals with a high genetic risk for diabetes but not in those with a low genetic risk. Especially, the genetic risk related to insulin resistance and liver lipid metabolism modulated the relationship between pancreas fat and insulin secretion (17). All these findings show how the effect of pancreas fat on T2D can be modified by many factors, including genetic risk, metabolic state, and other interacting fat compartments (7; 8). Co-culture models suggest the presence of a complex organ-organ crosstalk modulating insulin secretion (16; 39). K-means clustering revealed a fat-distribution pattern that might fuel such a detrimental inter-organ crosstalk. Specifically, individuals in the Pancreatic steatosis cluster had lower insulin secretion than expected for their degree of insulin resistance. The hypothesis that pancreatic fat exerts its detrimental effects in combination with other factors is further supported by interactions between fat in the pancreas and in the other tested compartments in terms of glycemia and diabetes risk.

One interesting finding of our current analysis is the contribution of muscle fat to the fat distribution patterns that are associated with T2D risk. The relations among muscle fat accumulation, insulin resistance, and T2D are complex (40). While several cross-sectional analyses suggested that muscle fat can be a risk factor for insulin resistance and T2D (9; 10; 13), it is well known that fat also accumulates in the muscle of athletes who are very insulin-sensitive (13; 40). Most prior studies evaluated muscle fat in the lower extremities, but here we quantified fat in trunk muscle (41). In concert with fat at other locations, fat in trunk muscle appears to link to T2D risk via muscle and systemic insulin resistance (13). A few previous studies have already looked at lower extremity muscle fat when analyzing body fat distribution patterns and T2D. Miljkovic et al. (10) simultaneously evaluated liver fat, muscle fat, and visceral fat in non-obese individuals. They showed that liver fat and muscle fat were associated with concurrent T2D. Unlike in the present study, in that study *incident* T2D was not evaluated, and pancreas fat was not measured. In another recent study (42), subgroups defined by fat accumulation were identified and were found to be associated with T2D, but that study was also cross-sectional, and pancreas fat was not evaluated.

Besides comprehensively investigating multiple fat compartments that are known to affect T2D pathogenesis, we aimed to address organ-organ interplay with our clustering approach (16; 39). This approach bore fruit, with the finding of interactions between fat compartments for glycemia and T2D risk. Furthermore, the clusters identified in this study had specific constellations of fat distribution and were strongly linked to T2D risk, likely via differences in insulin sensitivity and

insulin secretion. Further studies are warranted to uncover the detailed mechanisms of interplay among fat in different locations.

One limitation of this study is the fact that the cohorts were not population-based, so they might not reflect the general population. Moreover, we cannot exclude that fat accumulation in the analyzed trunk muscle behaves differently to other muscle compartments. Furthermore, there was some loss to follow-up, with a follow-up rate of 85% in Japan.

In conclusion, using information on patterns of fat distribution, we identified four distinct groups of individuals. Of note, the pattern of fat distribution was strongly associated with insulin sensitivity, with insulin secretion, and with the likelihood of future T2D. Unlike separately investigating fat in each location, this new approach provides information on the interplay of excess fat in different locations. Our findings underline the importance of body fat distribution rather than general adiposity. They can provide a basis for more individualized approaches to preventing and treating T2D.

Acknowledgements

The authors thank Keita Numata from the System Development Section, Keijinkai Maruyama Clinic; Kunihiko Hayashi, Hiromitsu Yonezawa, Eiji Kazuta, Kimihiro Saito, Keiko Takasaki, and Miyuki Yoshioka from the Department of Radiology, Keijinkai Maruyama Clinic. They also thank Joseph Green for suggestions and comments on earlier versions of this manuscript.

This work was funded in part by the German Center for Diabetes Research (DZD, 01GI0925), by the state of Baden-Württemberg (32-5400/58/2, Forum Gesundheitsstandort Baden-Württemberg), and by JSPS KAKENHI Grant Number JP19K16978 and JP22K15685.

Parts of this study were presented in abstract form at the 82th Scientific Sessions of the American Diabetes Association, New Orleans, LA, 3–7 June 2022.

Conflicts of interest: R.W. reports lecture fees from Novo Nordisk and Sanofi. R.W. served on an advisory board for Akcea Therapeutics, Daiichi Sankyo, Sanofi and NovoNordisk. M.H. reports research grants from Boehringer Ingelheim and Sanofi (both to the University Hospital of Tübingen) and lecture fees from Amryt, Novo Nordisk and Boehringer Ingelheim. He also served on an advisory board for Boehringer Ingelheim. All other authors have no potential conflicts of interest associated with this study.

Author contributions: *H.Y., R.W., and M.H.* designed the study. *S.T., J.M., T.H., M.D., N.H. and Y.K.* collected the data. *H.Y., R.W., and M.H.* wrote the draft. *H.Y., J.M., T.H., and R.W.* analyzed the data. *H.Y., S.T., J.M., T.H., Y.Y., M.D., N.H., Y.K., A.K., N.S., A.F., A.L.B., R.W., and M.H.*

reviewed, made critical revisions, and approved the article before submission. **H.Y.** is the guarantor for the Japanese data. **R.W., and M.H.** are the guarantors for the German data. As such, they had full access to all the data in the study and take responsibility for the integrity of the data and the accuracy of the data analysis.

References

1. Cefalu WT, Andersen DK, Arreaza-Rubin G, Pin CL, Sato S, Verchere CB, Woo M, Rosenblum ND: Heterogeneity of Diabetes: beta-Cells, Phenotypes, and Precision Medicine: Proceedings of an International Symposium of the Canadian Institutes of Health Research's Institute of Nutrition, Metabolism and Diabetes and the U.S. National Institutes of Health's National Institute of Diabetes and Digestive and Kidney Diseases. *Diabetes* 2022;71:1-22
2. Stefan N: Causes, consequences, and treatment of metabolically unhealthy fat distribution. *Lancet Diabetes Endocrinol* 2020;8:616-627
3. Wander PL, Boyko EJ, Leonetti DL, McNeely MJ, Kahn SE, Fujimoto WY: Change in visceral adiposity independently predicts a greater risk of developing type 2 diabetes over 10 years in Japanese Americans. *Diabetes care* 2013;36:289-293
4. Yamazaki H, Tsuboya T, Tsuji K, Dohke M, Maguchi H: Independent Association Between Improvement of Nonalcoholic Fatty Liver Disease and Reduced Incidence of Type 2 Diabetes. *Diabetes care* 2015;38:1673-1679
5. Yamazaki H, Wang J, Tauchi S, Dohke M, Hanawa N, Katanuma A, Saisho Y, Kamitani T, Fukuhara S, Yamamoto Y: Inverse Association Between Fatty Liver at Baseline Ultrasonography and Remission of Type 2 Diabetes Over a 2-Year Follow-up Period. *Clinical Gastroenterology and Hepatology* 2021;19:556-564

6. Martin S, Sorokin EP, Thomas EL, Sattar N, Cule M, Bell JD, Yaghootkar H: Estimating the Effect of Liver and Pancreas Volume and Fat Content on Risk of Diabetes: A Mendelian Randomization Study. *Diabetes care* 2022;45:460-468
7. Yamazaki H, Tauchi S, Wang J, Dohke M, Hanawa N, Kodama Y, Katanuma A, Saisho Y, Kamitani T, Fukuhara S, Yamamoto Y: Longitudinal association of fatty pancreas with the incidence of type-2 diabetes in lean individuals: a 6-year computed tomography-based cohort study. *Journal of gastroenterology* 2020;55:712-721
8. Wagner R, Eckstein SS, Yamazaki H, Gerst F, Machann J, Jaghutriz BA, Schurmann A, Solimena M, Singer S, Konigsrainer A, Birkenfeld AL, Haring HU, Fritsche A, Ullrich S, Heni M: Metabolic implications of pancreatic fat accumulation. *Nature reviews Endocrinology* 2022;18:43-54
9. Correa-de-Araujo R, Addison O, Miljkovic I, Goodpaster BH, Bergman BC, Clark RV, Elena JW, Esser KA, Ferrucci L, Harris-Love MO, Kritchevsky SB, Lorbergs A, Shepherd JA, Shulman GI, Rosen CJ: Myosteatorsis in the Context of Skeletal Muscle Function Deficit: An Interdisciplinary Workshop at the National Institute on Aging. *Front Physiol* 2020;11:963
10. Miljkovic I, Kuipers AL, Cvejkus RK, Carr JJ, Terry JG, Thyagarajan B, Wheeler VW, Nair S, Zmuda JM: Hepatic and Skeletal Muscle Adiposity Are Associated with Diabetes Independent of Visceral Adiposity in Nonobese African-Caribbean Men. *Metab Syndr Relat Disord* 2020;18:275-283
11. Neeland IJ, Poirier P, Despres JP: Cardiovascular and Metabolic Heterogeneity of Obesity: Clinical Challenges and Implications for Management. *Circulation* 2018;137:1391-1406

12. Mantovani A, Byrne CD, Bonora E, Targher G: Nonalcoholic Fatty Liver Disease and Risk of Incident Type 2 Diabetes: A Meta-analysis. *Diabetes care* 2018;41:372-382
13. Petersen MC, Shulman GI: Mechanisms of Insulin Action and Insulin Resistance. *Physiol Rev* 2018;98:2133-2223
14. Petrov MS, Taylor R: Intra-pancreatic fat deposition: bringing hidden fat to the fore. *Nature reviews Gastroenterology & hepatology* 2022;19:153-168
15. Brons C, Grunnet LG: MECHANISMS IN ENDOCRINOLOGY: Skeletal muscle lipotoxicity in insulin resistance and type 2 diabetes: a causal mechanism or an innocent bystander? *European journal of endocrinology* 2017;176:R67-R78
16. Gerst F, Wagner R, Kaiser G, Panse M, Heni M, Machann J, Bongers MN, Sartorius T, Sipos B, Fend F, Thiel C, Nadalin S, Konigsrainer A, Stefan N, Fritsche A, Haring HU, Ullrich S, Siegel-Axel D: Metabolic crosstalk between fatty pancreas and fatty liver: effects on local inflammation and insulin secretion. *Diabetologia* 2017;60:2240-2251
17. Wagner R, Jaghutriz BA, Gerst F, Barroso Oquendo M, Machann J, Schick F, Loffler MW, Nadalin S, Fend F, Konigsrainer A, Peter A, Siegel-Axel D, Ullrich S, Haring HU, Fritsche A, Heni M: Pancreatic Steatosis Associates With Impaired Insulin Secretion in Genetically Predisposed Individuals. *The Journal of clinical endocrinology and metabolism* 2020;105:3518-3525
18. Chan TT, Tse YK, Shun Lui RN, Hung Wong GL, Ling Chim AM, Shan Kong AP, Woo J, Wai Yeung DK, Abrigo JM, Wing Chu WC, Sun Wong VW, Yan Tang RS: Fatty pancreas is independently

associated with subsequent diabetes mellitus development: A 10-year prospective cohort study.

Clinical Gastroenterology and Hepatology 2021;<https://doi.org/10.1016/j.cgh.2021.09.027>

19. Barlow WE, Ichikawa L, Rosner D, Izumi S: Analysis of case-cohort designs. *J Clin Epidemiol* 1999;52:1165-1172

20. Breslow NE, Lumley T, Ballantyne CM, Chambless LE, Kulich M: Using the whole cohort in the analysis of case-cohort data. *American journal of epidemiology* 2009;169:1398-1405

21. Yamashita Y, Murayama S, Okada M, Watanabe Y, Kataoka M, Kaji Y, Imamura K, Takehara Y, Hayashi H, Ohno K, Awai K, Hirai T, Kojima K, Sakai S, Matsunaga N, Murakami T, Yoshimitsu K, Gabata T, Matsuzaki K, Tohno E, Kawahara Y, Nakayama T, Monzawa S, Takahashi S: The essence of the Japan Radiological Society/Japanese College of Radiology Imaging Guideline. *Jpn J Radiol* 2016;34:43-79

22. Kulathinal S, Karvanen J, Saarela O, Kuulasmaa K: Case-cohort design in practice - experiences from the MORGAM Project. *Epidemiol Perspect Innov* 2007;4:15

23. Babbar R, Heni M, Peter A, Hrabě de Angelis M, Häring H-U, Fritsche A, Preissl H, Schölkopf B, Wagner R: Prediction of Glucose Tolerance without an Oral Glucose Tolerance Test. *Frontiers in endocrinology* 2018;9

24. Kodama Y, Ng CS, Wu TT, Ayers GD, Curley SA, Abdalla EK, Vauthey JN, Charnsangavej C: Comparison of CT methods for determining the fat content of the liver. *AJR American journal of roentgenology* 2007;188:1307-1312

25. Kim SY, Kim H, Cho JY, Lim S, Cha K, Lee KH, Kim YH, Kim JH, Yoon YS, Han HS, Kang HS: Quantitative assessment of pancreatic fat by using unenhanced CT: pathologic correlation and clinical implications. *Radiology* 2014;271:104-112
26. Schweitzer L, Geisler C, Pourhassan M, Braun W, Gluer CC, Bosy-Westphal A, Muller MJ: What is the best reference site for a single MRI slice to assess whole-body skeletal muscle and adipose tissue volumes in healthy adults? *The American journal of clinical nutrition* 2015;102:58-65
27. Cespedes Feliciano EM, Popuri K, Cobzas D, Baracos VE, Beg MF, Khan AD, Ma C, Chow V, Prado CM, Xiao J, Liu V, Chen WY, Meyerhardt J, Albers KB, Caan BJ: Evaluation of automated computed tomography segmentation to assess body composition and mortality associations in cancer patients. *J Cachexia Sarcopenia Muscle* 2020;11:1258-1269
28. Faron A, Sprinkart AM, Kuetting DLR, Feisst A, Isaak A, Endler C, Chang J, Nowak S, Block W, Thomas D, Attenberger U, Luetkens JA: Body composition analysis using CT and MRI: intra-individual intermodal comparison of muscle mass and myosteatosis. *Scientific reports* 2020;10:11765
29. Goodpaster BH, Kelley DE, Thaete FL, He J, Ross R: Skeletal muscle attenuation determined by computed tomography is associated with skeletal muscle lipid content. *J Appl Physiol* (1985) 2000;89:104-110
30. Machann J, Thamer C, Stefan N, Schwenzer NF, Kantartzis K, Haring HU, Claussen CD, Fritsche A, Schick F: Follow-up whole-body assessment of adipose tissue compartments during a lifestyle intervention in a large cohort at increased risk for type 2 diabetes. *Radiology* 2010;257:353-363

31. Wurslin C, Machann J, Rempp H, Claussen C, Yang B, Schick F: Topography mapping of whole body adipose tissue using A fully automated and standardized procedure. *Journal of magnetic resonance imaging* : JMRI 2010;31:430-439
32. Machann J, Hasenbalg M, Dienes J, Wagner R, Sandforth A, Fritz V, Birkenfeld AL, Nikolaou K, Kullmann S, Schick F, Heni M: Short-Term Variability of Proton Density Fat Fraction in Pancreas and Liver Assessed by Multiecho Chemical-Shift Encoding-Based MRI at 3 T. *Journal of magnetic resonance imaging* : JMRI 2022;<https://doi.org/10.1002/jmri.28084>
33. Isensee F, Jaeger PF, Kohl SAA, Petersen J, Maier-Hein KH: nnU-Net: a self-configuring method for deep learning-based biomedical image segmentation. *Nat Methods* 2021;18:203-211
34. Hudak S, Huber P, Lamprinou A, Fritsche L, Stefan N, Peter A, Birkenfeld AL, Fritsche A, Heni M, Wagner R: Reproducibility and discrimination of different indices of insulin sensitivity and insulin secretion. *PloS one* 2021;16:e0258476
35. Hoffmann C, Schneeweiss P, Randrianarisoa E, Schnauder G, Kappler L, Machann J, Schick F, Fritsche A, Heni M, Birkenfeld A, Niess AM, Haring HU, Weigert C, Moller A: Response of Mitochondrial Respiration in Adipose Tissue and Muscle to 8 Weeks of Endurance Exercise in Obese Subjects. *The Journal of clinical endocrinology and metabolism* 2020;105:e4023-e4037
36. Charrad M, Ghazzali N, Boiteau V, Niknafs A: NbClust: An R Package for Determining the Relevant Number of Clusters in a Data Set. *Journal of Statistical Software* 2014;61:1-36
37. Meex RCR, Watt MJ: Hepatokines: linking nonalcoholic fatty liver disease and insulin resistance.

Nature reviews Endocrinology 2017;13:509-520

38. Stefan N, Cusi K: A global view of the interplay between non-alcoholic fatty liver disease and diabetes. *Lancet Diabetes Endocrinol* 2022;[https://doi.org/10.1016/S2213-8587\(22\)00003-1](https://doi.org/10.1016/S2213-8587(22)00003-1)

39. Gerst F, Wagner R, Oquendo MB, Siegel-Axel D, Fritsche A, Heni M, Staiger H, Haring HU, Ullrich S: What role do fat cells play in pancreatic tissue? *Mol Metab* 2019;25:1-10

40. Gilbert M: Role of skeletal muscle lipids in the pathogenesis of insulin resistance of obesity and type 2 diabetes. *Journal of diabetes investigation* 2021;12:1934-1941

41. Maltais A, Almeras N, Lemieux I, Tremblay A, Bergeron J, Poirier P, Despres JP: Trunk muscle quality assessed by computed tomography: Association with adiposity indices and glucose tolerance in men. *Metabolism: clinical and experimental* 2018;85:205-212

42. Linge J, Whitcher B, Borga M, Dahlqvist Leinhard O: Sub-phenotyping Metabolic Disorders Using Body Composition: An Individualized, Nonparametric Approach Utilizing Large Data Sets. *Obesity* 2019;27:1190-1199

Table 1. Baseline characteristics

	Japan		P-value	Germany
	Non-cases (n = 608)	Cases (n = 146)		Total (n = 319)
Age (years)	51 (43-59)	54 (47-59)	0.009	44 (34-60)
Male, n (%)	440 (72.4)	128 (87.7)	< 0.001	87 (27.3%)
Body mass index (kg/m ²)	23.5 (21.6-25.8)	25.7 (23.6-28.7)	< 0.001	27.0 (23.0-31.5)
CT-based indicators				
Liver fat (HU)	65.1 (60.4-68.4)	59.7 (49.4-65.2)	< 0.001	N/A
Pancreas fat (HU)	48.8 (43.4-52.3)	44.6 (39.1-48.5)	< 0.001	N/A
Muscle fat (HU)	40.8 (36.1-44.9)	39.3 (35.9-42.7)	0.009	N/A
Visceral fat (cm ²)	86.3 (37.7-142.5)	156.1 (109.6-206.0)	< 0.001	N/A
Muscle area (cm ²)	142.8 (110.5-161.6)	158.2 (138.8-174.8)	< 0.001	N/A
MRI-based indicators				
Liver fat (%)	N/A	N/A		2.2 (0.8-5.8)
Pancreas fat (%)	N/A	N/A		3.5 (1.9-6.3)
Muscle fat (%)	N/A	N/A		7.1 (5.8-8.6)
Visceral fat (L)	N/A	N/A		2.6 (1.5-4.4)
Muscle area (cm ²)	N/A	N/A		134.9 (123.1-158.7)
Fasting plasma glucose (mg/dL)	90.0 (84.0-95.0)	106.0 (97.0-113.0)	< 0.001	91.8 (84.6-97.2)
Fasting plasma glucose (mmol/L)	5.0 (4.7-5.3)	5.9 (5.4-6.3)	< 0.001	5.1 (4.7-5.4)
HbA1c (%)	5.3 (5.1-5.4)	5.8 (5.5-6.0)	< 0.001	5.5 (5.3-5.8)
HbA1c (mmol/mol)	34 (32-36)	40 (37-42)	< 0.001	37 (34-40)
Triglycerides (mg/dL)	92.0 (64.5-132.5)	122.5 (87.0-190.0)	< 0.001	91.0 (65.0-123.0)
HDL cholesterol (mg/dL)	57.0 (48.0-67.0)	51.0 (44.0-59.0)	< 0.001	54.0 (46.0-66.0)
LDL cholesterol (mg/dL)	120.0 (102.0-140.5)	130.0 (102.0-153.0)	0.025	115.0 (97.0-142.0)
Systolic blood pressure (mmHg)	120.0 (110.0-130.0)	125.0 (120.0-136.0)	< 0.001	130.0 (118.0-141.0)
Diastolic blood pressure (mmHg)	76.0 (70.0-81.0)	80.0 (72.0-88.0)	< 0.001	84.0 (77.0-92.0)
Current smoker, n (%)	176 (28.9)	53 (36.3)	0.089	22 (7.2)

Alcohol intake, n (%)	213 (35.0)	51 (34.9)	1.00	14 (4.6)
Family history of diabetes, n (%)	120 (19.7)	36 (24.7)	0.21	180 (56.4)
Antihypertensive drug, n (%)	82 (13.5)	47 (32.2)	< 0.001	18 (5.6)
Lipid-lowering drug, n (%)	67 (11.0)	23 (15.8)	0.12	7 (2.2)

Continuous data are expressed as medians and interquartile ranges. Fisher’s exact test and Wilcoxon’s rank-sum tests were used to compare non-cases with cases in Japan.

Missing data: muscle volume (n = 9), systolic blood pressure (n = 1), diastolic blood pressure (n = 1), current smoker (n = 14), alcohol intake (n = 13)

HU, Hounsfield unit

Table 2. Hazard ratios and 95% confidence intervals for the association between membership in a fat-distribution cluster at baseline and the incidence of diabetes mellitus, from the case-cohort study in Japan (n = 754)

	Cluster 1 Hepatic steatosis	Cluster 2 Pancreatic steatosis	Cluster 3 Trunk myosteatosi	Cluster 4 Steatopenia
Subcohort, n (%)	118 (17.9)	62 (9.4)	224 (34.0)	254 (38.6)
Cases of type-2 diabetes*, n (%)	56 (38.4)	23 (15.8)	44 (30.1)	23 (15.8)
HR (95% CI), P-value				
Unadjusted analysis	5.49 (3.25-9.27), < 0.001	5.15 (2.73-9.71), < 0.001	2.36 (1.38-4.01), 0.002	1.00 (reference)
Age-and-sex-adjusted analysis	5.15 (3.02-8.79), < 0.001	3.74 (1.85-7.57), < 0.001	1.98 (1.09-3.58), 0.024	1.00 (reference)
Multivariable-adjusted model 1	4.02 (2.27-7.12), < 0.001	3.38 (1.65-6.91), 0.001	1.95 (1.07-3.54), 0.029	1.00 (reference)
Multivariable-adjusted model 2	3.23 (1.69-6.15), < 0.001	2.65 (1.20-5.87), 0.016	1.76 (0.96-3.24), 0.068	1.00 (reference)
Multivariable-adjusted model 3	3.23 (1.62-6.44), 0.001	2.52 (1.12-5.67), 0.026	1.65 (0.88-3.10), 0.12	1.00 (reference)

Weighted Cox regression analyses were conducted to estimate the hazard ratios, 95% confidence intervals, and P-values.

Model 1: Adjusted for age, sex, alcohol intake, current smoking, and muscle area

Model 2: Adjusted for age, sex, alcohol intake, current smoking, muscle area, and body mass index

Model 3: Adjusted for age, sex, alcohol intake, current smoking, muscle area, and body mass index, systolic blood pressure, diastolic blood pressure, triglycerides, HDL-cholesterol, LDL-cholesterol, antihypertensive drugs, and lipid-lowering drugs

HR, hazard ratio; CI, confidence interval

*Includes cases within and outside of the randomly selected subcohort.

Table 3. Glycemia, insulin sensitivity, and insulin secretion based on results of 75 g oral glucose tolerance tests, across fat-distribution clusters in Germany (n = 319)

	Cluster 1 Hepatic steatosis (n = 39)	Cluster 2 Pancreatic steatosis (n = 21)	Cluster 3 Trunk myosteatosis (n = 103)	Cluster 4 Steatopenia (n = 156)
Glycemia				
AUC Glucose ₀₋₁₂₀	1038.9 (969.4-1108.4)	980.7 (905.1-1056.4)	956.5 (920.7-992.3)	806.7 (777.3-836.1)
P-values	< 0.001	< 0.001	< 0.001	reference
Insulin sensitivity				
NEFA-ISI	2.1 (1.9-2.3)	3.0 (2.3-3.8)	3.4 (3.1-3.6)	5.5 (5.2-5.8)
P-values	< 0.001	< 0.001	< 0.001	reference
Insulin secretion				
AUC C-peptide ₀₋₃₀ /AUC Glucose ₀₋₃₀	215.8 (194.4-237.2)	169.2 (138.2-200.1)	170.3 (158.2-182.5)	145.7 (137.1-154.2)
P-values	< 0.001	0.12	< 0.001	Reference
Sensitivity-adjusted insulin secretion				
AUC C-peptide ₀₋₃₀ /AUC Glucose ₀₋₃₀ residuals	9.7 (-9.1-28.5)	-15.2 (-37.2-6.8)	-5.9 (-16.8-5.1)	3.2 (-4.8-11.2)
P-values	0.57	0.081	0.081	reference

Mean and 95% confidence intervals are shown. The unit of AUC Glucose₀₋₁₂₀ is mmol*min/ml. Insulin sensitivity and secretion are in arbitrary units. P-values were calculated from Wilcoxon's rank-sum tests comparing the Steatopenia cluster with the other clusters. To estimate insulin

secretion adjusted for insulin sensitivity, we calculated $\text{AUC C-peptide}_{0-30}/\text{AUC Glucose}_{0-30}$ residuals from the regression of $\text{AUC C-peptide}_{0-30}/\text{AUC Glucose}_{0-30}$ on NEFA-ISI and its quadratic term.

Missing data: Insulin sensitivity (n = 3), Insulin secretion (n = 4), sensitivity-adjusted insulin secretion (n = 7)

AUC, area under the curve; NEFA-ISI, non-esterified fatty acids-based insulin sensitivity index

Figure legends

Figure 1. K-means clustering of fat distribution

Distributions of visceral fat, liver fat, pancreas fat, and muscle fat are shown.

K-means clustering resulted in four clusters: a Hepatic steatosis cluster (Cluster 1), a Pancreatic steatosis cluster (Cluster 2), a Trunk myosteatosis cluster (Cluster 3), and a Steatopenia cluster (Cluster 4).

HU, Hounsfield unit

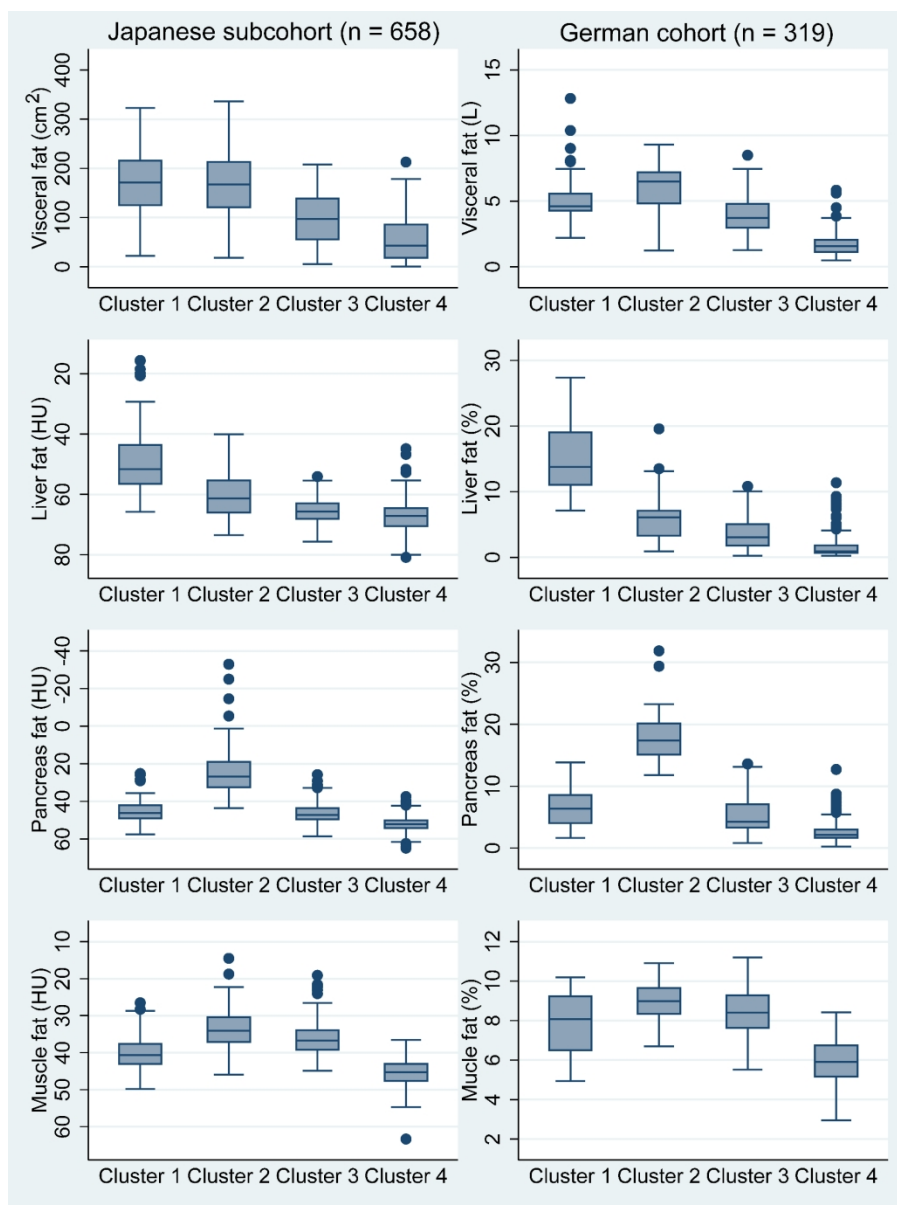


Figure 1. K-means clustering of fat distribution
Distributions of visceral fat, liver fat, pancreas fat, and muscle fat are shown.
K-means clustering resulted in four clusters: a Hepatic steatosis cluster (Cluster 1), a Pancreatic steatosis cluster (Cluster 2), a Trunk myosteatosis cluster (Cluster 3), and a Steatopenia cluster (Cluster 4).
HU, Hounsfield unit

228x304mm (600 x 600 DPI)

Supplementary Table 1. Baseline characteristics of the randomly selected subcohort (Japan, n = 658), by fat-distribution cluster

	Cluster 1 Hepatic steatosis (n = 118)	Cluster 2 Pancreatic steatosis (n = 62)	Cluster 3 Trunk myosteatosi (n = 224)	Cluster 4 Steatopenia (n = 254)	P-value
Age (years)	50 (43-57)	61 (55-64)	56 (50-60)	45 (40-53)	< 0.001
Male, n (%)	92 (78.0)	49 (79.0)	160 (71.4)	183 (72.0)	0.42
Body mass index (kg/m ²)	26.6 (24.7-29.0)	26.1 (24.3-27.6)	23.5 (22.1-25.4)	22.3 (20.6-23.9)	< 0.001
Height (cm)	167.0 (160.9-171.0)	165.5 (159.5-170.4)	166.3 (160.4-170.9)	167.4 (161.2-172.7)	0.17
Weight (kg)	75.1 (67.6-83.9)	71.7 (64.9-77.9)	65.1 (56.8-72.5)	63.2 (54.1-70.0)	<0.001
Waist circumference (cm)	92.4 (87.0-98.5)	92.5 (88.5-96.5)	85.7 (82.0-90.5)	80.6 (75.9-85.0)	<0.001
Liver fat (HU)	51.6 (43.3-56.8)	61.4 (55.0-66.3)	65.6 (62.7-68.4)	67.2 (64.3-70.9)	< 0.001
Pancreas fat (HU)	46.3 (41.5-49.5)	26.8 (18.5-33.0)	47.2 (43.2-50.1)	52.1 (49.7-54.6)	< 0.001
Muscle fat (HU)	40.7 (37.4-43.3)	34.1 (30.2-37.4)	36.8 (33.7-39.5)	45.3 (42.8-47.8)	< 0.001
Visceral fat (cm ²)	171.0 (123.5-217.6)	167.1 (118.9-215.0)	96.8 (53.4-140.1)	42.7 (16.2-87.8)	< 0.001
Muscle area (cm ²)	160.7 (139.0-173.2)	148.3 (123.3-161.5)	138.4 (105.5-155.9)	140.8 (108.9-161.1)	< 0.001
Fasting plasma glucose (mg/dL)	93.0 (87.0-101.0)	94.5 (90.0-98.0)	91.0 (86.5-96.0)	88.0 (81.0-93.0)	< 0.001
Fasting plasma glucose (mmol/L)	5.2 (4.8-5.6)	5.3 (5.0-5.4)	5.1 (4.8-5.3)	4.9 (4.5-5.2)	< 0.001
HbA1c (%)	5.4 (5.2-5.6)	5.4 (5.3-5.6)	5.3 (5.1-5.5)	5.2 (5.0-5.4)	< 0.001
HbA1c (mmol/mol)	36 (33-38)	36 (34-38)	34 (32-37)	33 (31-36)	< 0.001
Triglycerides (mg/dL)	134.0 (98.0-189.0)	121.5 (86.0-172.0)	88.0 (66.0-121.5)	79.5 (56.0-115.0)	< 0.001
HDL cholesterol (mg/dL)	51.0 (44.0-59.0)	51.0 (45.0-62.0)	57.0 (48.5-68.0)	59.0 (48.0-69.0)	< 0.001
LDL cholesterol (mg/dL)	125.5 (109.0-144.0)	129.0 (109.0-153.0)	125.0 (105.0-142.0)	115.0 (96.0-135.0)	< 0.001
Systolic blood pressure (mmHg)	124.0 (118.0-132.0)	120.0 (114.0-132.0)	120.0 (110.0-130.0)	112.0 (104.0-124.0)	< 0.001
Diastolic blood pressure (mmHg)	80.0 (74.0-86.0)	79.0 (70.0-84.0)	78.0 (70.0-84.0)	72.0 (68.0-80.0)	< 0.001
Current smoker, n (%)	36 (30.5)	11 (17.7)	59 (26.3)	90 (35.4)	0.023
Alcohol intake, n (%)	35 (29.7)	16 (25.8)	89 (39.7)	86 (33.9)	0.11
Physical activity, n (%)	15 (12.7)	16 (25.8)	51 (22.9)	56 (22.0)	0.077

Family history of diabetes, n (%)	23 (19.5)	16 (25.8)	39 (17.4)	56 (22.0)	0.40
Antihypertensive drug, n (%)	28 (23.7)	16 (25.8)	42 (18.8)	13 (5.1)	< 0.001
Lipid-lowering drug, n (%)	26 (22.0)	9 (14.5)	30 (13.4)	11 (4.3)	< 0.001

Continuous data are expressed as medians and interquartile ranges. Fisher's exact test was used for categorical data. The Kruskal-Wallis test was used for continuous data. We regarded participants who met all of the following criteria as “physically active”: length of each physical-exercise session ≥ 30 minutes, frequency of physical exercise ≥ 2 times a week, and duration of physical exercise ≥ 1 year. Missing data: waist circumference (n = 3), LDL-cholesterol (n = 2), physical activity (n = 1)

HU, Hounsfield unit

Supplementary Table 2. Baseline characteristics of the cohort in Germany (n = 319), by fat-distribution cluster

	Cluster 1 Hepatic steatosis (n = 39)	Cluster 2 Pancreatic steatosis (n = 21)	Cluster 3 Trunk myosteatosi (n = 103)	Cluster 4 Steatopenia (n = 156)	P-value
Age (years)	55 (40-62)	56 (49-64)	58 (43-65)	36 (29-44)	< 0.001
Male, n (%)	8 (20.5)	8 (38.1)	29 (28.2)	42 (26.9)	0.53
Body mass index (kg/m ²)	32.4 (29.7-35.2)	34.0 (29.7-39.7)	29.4 (25.9-32.7)	23.1 (21.1-26.5)	< 0.001
Height (cm)	164.8 (160.0-172.0)	170.0 (164.0-176.0)	168.0 (164.0-174.8)	168.0 (164.0-175.5)	0.16
Weight (kg)	88.9 (78.7-109.1)	105.5 (85.8-113.5)	82.4 (72.6-94.9)	67.5 (60.5-78.3)	<0.001
Waist circumference (cm)	99.0 (93.5-114.0)	113.5 (98.5-118.0)	96.0 (87.5-104.0)	78.0 (73.0-86.0)	<0.001
Liver fat (%)	13.8 (10.9-19.2)	6.1 (3.2-7.2)	3.0 (1.6-5.2)	0.9 (0.6-2.0)	< 0.001
Pancreas fat (%)	6.4 (3.9-8.7)	17.4 (15.0-20.3)	4.3 (3.2-7.2)	2.2 (1.5-3.1)	< 0.001
Muscle fat (%)	8.1 (6.4-9.3)	9.0 (8.3-9.7)	8.4 (7.6-9.3)	5.9 (5.1-6.8)	< 0.001
Visceral fat (L)	4.6 (4.2-5.6)	6.5 (4.8-7.3)	3.7 (2.9-4.8)	1.6 (1.0-2.1)	< 0.001
Muscle area (cm ²)	140.2 (128.4-168.1)	145.5 (131.6-206.7)	138.5 (122.8-161.0)	129.8 (121.8-148.8)	0.015
Fasting plasma glucose (mg/dL)	93.6 (91.8-100.8)	95.4 (91.8-100.8)	95.4 (90.0-100.8)	86.4 (82.8-91.8)	< 0.001
Fasting plasma glucose (mmol/L)	5.2 (5.1-5.6)	5.3 (5.1-5.6)	5.3 (5.0-5.6)	4.8 (4.6-5.1)	< 0.001
HbA1c (%)	5.7 (5.3-6.0)	5.6 (5.3-6.0)	5.7 (5.4-5.9)	5.4 (5.2-5.6)	< 0.001
HbA1c (mmol/mol)	39 (34-42)	38 (34-42)	39 (36-41)	36 (33-38)	< 0.001
Triglycerides (mg/dL)	117.0 (92.0-161.0)	123.0 (96.0-155.0)	98.0 (77.0-136.0)	72.0 (56.0-97.5)	< 0.001
HDL cholesterol (mg/dL)	48.0 (41.0-58.0)	53.0 (47.0-58.0)	54.0 (45.0-67.0)	55.5 (48.0-69.5)	0.002
LDL cholesterol (mg/dL)	124.0 (105.0-158.0)	145.0 (120.0-163.0)	125.0 (108.0-157.0)	104.5 (90.0-125.0)	< 0.001
Systolic blood pressure (mmHg)	136.0 (125.0-151.0)	141.0 (135.0-145.0)	134.0 (124.0-144.0)	124.0 (115.0-134.0)	< 0.001
Diastolic blood pressure (mmHg)	89.0 (82.0-101.0)	90.0 (86.0-97.0)	86.0 (80.0-95.0)	82.0 (74.0-90.0)	< 0.001
Current smoker, n (%)	4 (10.5)	0 (0.0)	5 (5.2)	13 (8.7)	0.39
Alcohol intake, n (%)	3 (7.9)	4 (19.0)	4 (4.1)	3 (2.0)	0.007
Habitual physical activity score*	8.2 (7.0-9.0)	7.8 (6.9-8.4)	8.5 (7.1-9.4)	8.1 (7.3-9.0)	0.25

Family history of diabetes, n (%)	25 (64.1)	14 (66.7)	62 (60.2)	79 (50.6)	0.21
Antihypertensive drug, n (%)	2 (5.1)	2 (9.5)	7 (6.8)	7 (4.5)	0.59
Lipid-lowering drug, n (%)	0 (0.0)	0 (0.0)	3 (2.9)	4 (2.6)	0.85

Continuous data are expressed as medians and interquartile ranges. Fisher's exact test was used for categorical data. The Kruskal-Wallis test was used for continuous data.

Missing data: muscle volume (n = 9), systolic blood pressure (n = 1), diastolic blood pressure (n = 1), current smoker (n = 14), alcohol intake (n = 13), habitual physical activity score (n = 17)

* J A Baecke, J Burema, J E Frijters. A short questionnaire for the measurement of habitual physical activity in epidemiological studies. *Am J Clin Nutr.* 1982;36(5):936-42.

Supplementary Table 3. Hazard ratios and 95% confidence intervals for pairwise comparisons: the association between membership in a fat-distribution cluster at baseline and the incidence of diabetes mellitus, from the case-cohort study in Japan (n = 754)

HRs (95% CIs), P-values	Cluster 1 vs Cluster 3*	Cluster 2 vs Cluster 3*	Cluster 1 vs Cluster 2*
Unadjusted analysis	2.33 (1.49-3.64), < 0.001	2.19 (1.24-3.87), 0.007	1.07 (0.61-1.87), 0.82
Age-and-sex-adjusted analysis	2.60 (1.61-4.21), < 0.001	1.89 (1.05-3.39), 0.033	1.38 (0.75-2.52), 0.30
Multivariable-adjusted model 1	2.06 (1.26-3.39), 0.004	1.73 (0.96-3.13), 0.067	1.19 (0.65-2.19), 0.58
Multivariable-adjusted model 2	1.83 (1.08-3.10), 0.024	1.51 (0.80-2.83), 0.20	1.22 (0.66-2.25), 0.53
Multivariable-adjusted model 3	1.96 (1.11-3.44), 0.020	1.52 (0.80-2.90), 0.20	1.28 (0.67-2.46), 0.45

*The reference cluster for each comparison.

Cluster 1: Hepatic steatosis, Cluster 2: Pancreatic steatosis, Cluster 3: Trunk myosteatorsis

Pairwise comparisons in addition to table 2 in the main manuscript are shown.

Weighted Cox regression analyses were conducted to estimate the hazard ratios, 95% confidence intervals, and P-values.

Model 1: Adjusted for age, sex, alcohol intake, current smoking, and muscle area

Model 2: Adjusted for age, sex, alcohol intake, current smoking, muscle area, and body mass index

Model 3: Adjusted for age, sex, alcohol intake, current smoking, muscle area, body mass index, systolic blood pressure, diastolic blood pressure, triglycerides, HDL-cholesterol, LDL-cholesterol, antihypertensive drugs, and lipid-lowering drugs

Supplementary Table 4. Pairwise interactions of fat compartments regarding type-2 diabetes risk (Japan, n = 754)

HR (95% CI), P-value	Visceral fat (per 1 SD)	Liver fat (per 1 SD)	Pancreas fat (per 1 SD)
Liver fat (per 1 SD)	Visceral fat: 1.76 (1.46-2.13), < 0.001 Liver fat: 1.53 (1.23-1.91), < 0.001 Interaction: 0.90 (0.78-1.04), 0.17		
Pancreas fat (per 1 SD)	Visceral fat: 1.98 (1.65-2.39), < 0.001 Pancreas fat: 1.48 (1.18-1.86), 0.001 Interaction: 0.79 (0.67-0.93), 0.004	Liver fat: 1.69 (1.48-1.92), < 0.001 Pancreas fat: 1.36 (1.16-1.59), < 0.001 Interaction: 0.88 (0.78-1.00), 0.055	
Muscle fat (per 1 SD)	Visceral fat: 1.99 (1.69-2.35), < 0.001 Muscle fat: 1.23 (1.02-1.48), 0.029 Interaction: 0.93 (0.82-1.06), 0.26	Liver fat: 1.68 (1.47-1.92), < 0.001 Muscle fat: 1.27 (1.07-1.50), 0.006 Interaction: 1.02 (0.90-1.17), 0.71	Pancreas fat: 1.48 (1.29-1.69), < 0.001 Muscle fat: 1.23 (1.03-1.47), 0.020 Interaction: 0.77 (0.66-0.90), 0.001

Weighted Cox regression analyses were conducted to estimate the hazard ratios, 95% confidence intervals, and P-values for the association of fat deposits with incident type-2 diabetes.

Visceral fat area, liver attenuation, pancreas attenuation, and muscle attenuation were used as fat variables.

Liver attenuation, pancreas attenuation, and muscle attenuation were “flipped” such that higher value would correspond to more fat.

Each fat variable was standardized (mean = 0, SD = 1) and analyzed as a continuous variable.

Mean (1 SD): 100.7 (70.3) cm² for visceral fat, 62.8 (9.3) HU for liver fat, 46.1 (10.5) HU for pancreas fat, and 40.2 (6.3) HU for muscle fat.

SD, standard deviation; HR, hazard ratio; CI, confidence interval; HU, Hounsfield unit

Supplementary Table 5. P-values for pairwise comparisons: glycemia, insulin sensitivity, and insulin secretion based on results of 75g oral glucose tolerance tests, across fat-distribution clusters in Germany (n = 319)

P-values	Cluster 1 vs Cluster 3	Cluster 2 vs Cluster 3	Cluster 1 vs Cluster 2
Glycemia	0.022	0.55	0.27
Insulin sensitivity	< 0.001	0.087	0.016
Insulin secretion	< 0.001	0.79	0.010
Sensitivity-adjusted insulin secretion	0.15	0.49	0.091

Cluster 1: Hepatic steatosis, Cluster 2: Pancreatic steatosis, Cluster 3: Trunk myosteatosis

Pairwise comparisons in addition to table 3 in the main manuscript are shown.

P-values were calculated from Wilcoxon's rank-sum tests.

Supplementary Table 6. Pairwise interactions of fat compartments regarding glycemia (Germany, n = 319)

β (95% CI), P-value	Visceral fat (per 1 SD)	Liver fat (per 1 SD)	Pancreas fat (per 1 SD)
Liver fat (per 1 SD)	Visceral fat: 83.3 (58.6-108.0), < 0.001 Liver fat: 54.0 (25.7-82.3), < 0.001 Interaction: -23.6 (-40.0- -7.16), 0.005		
Pancreas fat (per 1 SD)	Visceral fat: 100.1 (76.7-123.5), < 0.001 Pancreas fat: 31.7 (4.53-58.8), 0.022 Interaction: -34.7 (-53.6- -15.7), < 0.001	Liver fat: 77.5 (54.8-100.1), < 0.001 Pancreas fat: 44.0 (20.7-67.3), < 0.001 Interaction: -23.4 (-41.0- -5.92), 0.009	
Muscle fat (per 1 SD)	Visceral fat: 95.0 (71.8-118.1), < 0.001 Muscle fat: 23.6 (0.93-46.3), 0.041 Interaction: -30.6 (-51.8- -9.35), 0.005	Liver fat: 70.5 (49.3-91.6), < 0.001 Muscle fat: 51.0 (30.0-72.0), < 0.001 Interaction: -9.83 (-30.0-10.4), 0.34	Pancreas fat: 65.4 (35.1-95.7), < 0.001 Muscle fat: 44.7 (20.5-68.9), < 0.001 Interaction: -36.4 (-58.7- -14.1), 0.001

Glycemia was evaluated by AUC Glucose₀₋₁₂₀ from a 75 g oral glucose tolerance test, and the unit is mmol*min/ml.

Multiple linear regression models were used to estimate β, 95% CI, and P-values for the associations of fat deposits with glycemia.

Each fat variable was standardized (mean = 0, SD = 1) and analyzed as a continuous variable.

Mean (1 SD): 3.1 (2.1) L for visceral fat, 4.3 (5.2) % for liver fat, 5.0 (4.8) % for pancreas fat, 7.1 (1.7) % for muscle fat, and 894.9 (207.1) mmol*min/ml for the AUC Glucose₀₋₁₂₀.

SD, standard deviation; CI, confidence interval; AUC, area under the curve

Downloaded from <http://diabetesjournals.org/diabetes/article-pdf/doi/10.2337/db22-0315/6846899/db220315.pdf> by HELMHOLTZ ZENTRUM MUENCHEN user on 08 July 2022

Supplementary Table 7. Regression coefficients (β) and 95% confidence intervals for the associations of fat deposits with insulin sensitivity, insulin secretion, and aerobic capacity (Germany, n = 319)

	Insulin sensitivity	Insulin secretion	Adjusted insulin secretion	Aerobic capacity
	β (95% CI), P-value	β (95% CI), P-value	β (95% CI), P-value	β (95% CI), P-value
Visceral fat (per 1 SD)	-1.29 (-1.47- -1.10), < 0.001	16.5 (9.72-23.2), < 0.001	-5.83 (-11.7-0.038), 0.052	-2.02 (-3.06- -0.98), < 0.001
Liver fat (per 1 SD)	-1.19 (-1.38- -1.00), < 0.001	21.9 (15.4-28.4), < 0.001	-0.25 (-6.08- 5.58), 0.93	-2.25 (-3.56- -0.95), 0.001
Pancreas fat (per 1 SD)	-0.74 (-0.95- -0.52), < 0.001	4.92 (-2.00-11.8), 0.16	-7.18 (-13.0- -1.37), 0.016	-1.02 (-2.03- -0.0017), 0.050
Muscle fat (per 1 SD)	-0.90 (-1.11- -0.70), < 0.001	9.41 (2.54-16.3), 0.007	-5.22 (-11.1-0.61), 0.079	-2.48 (-3.52- -1.44), < 0.001

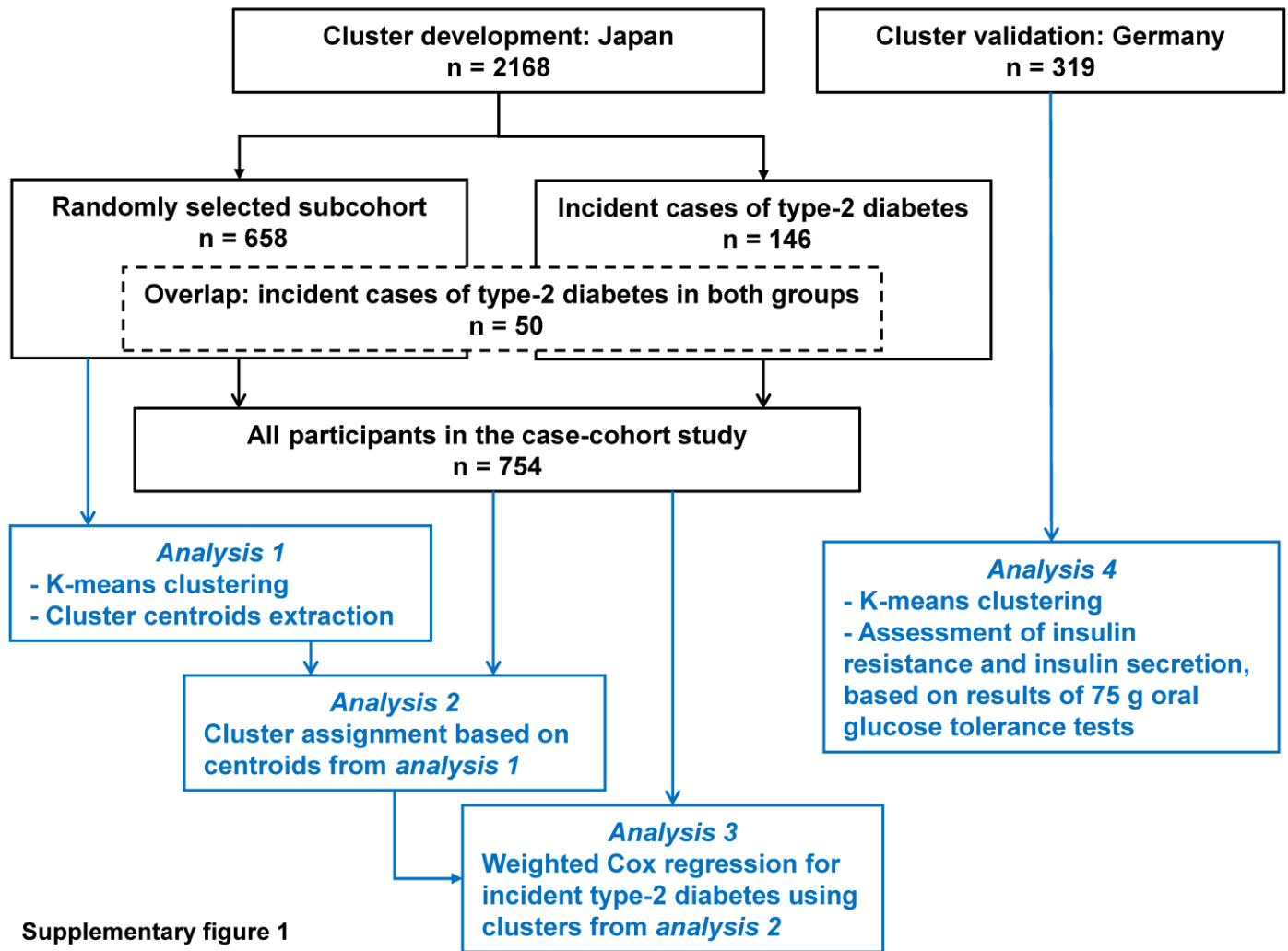
Insulin sensitivity and insulin secretion were assessed by NEFA-ISI and AUC C-peptide₀₋₃₀/AUC Glucose₀₋₃₀, respectively. To estimate insulin secretion adjusted for insulin sensitivity, we calculated AUC C-peptide₀₋₃₀/AUC Glucose₀₋₃₀ residuals from regression of AUC C-peptide₀₋₃₀/AUC Glucose₀₋₃₀ on NEFA-ISI and its quadratic term. Aerobic capacity was quantified as VO₂ max. Insulin sensitivity and secretion are in arbitrary units, and the unit of VO₂ max is mL/kg/min. Linear regression models were used to estimate β , 95% CI, and P-values. Each fat variable was standardized (mean = 0, SD = 1) and analyzed as a continuous variable.

Mean (1 SD): 3.1 (2.1) L for visceral fat, 4.3 (5.2) % for liver fat, 5.0 (4.8) % for pancreas fat, 7.1 (1.7) % for muscle fat, 4.3 (2.1) for NEFA-ISI, 163.7 (62.8) for the AUC C-peptide₀₋₃₀/AUC Glucose₀₋₃₀, 0 (52.6) for the AUC C-peptide₀₋₃₀/AUC Glucose₀₋₃₀ residuals, and 20.1 (6.2) mL/kg/min for the VO₂ max.

Missing data: insulin sensitivity (n = 3), sensitivity-adjusted insulin secretion (n = 7), aerobic capacity (n = 168)

SD, standard deviation; BMI, body mass index; NEFA-ISI, non-esterified fatty acids-based insulin sensitivity index; AUC, area under the curve;

VO₂ max, maximal oxygen uptake



Supplementary figure 1

Supplementary Figure 1. Study flow diagram.

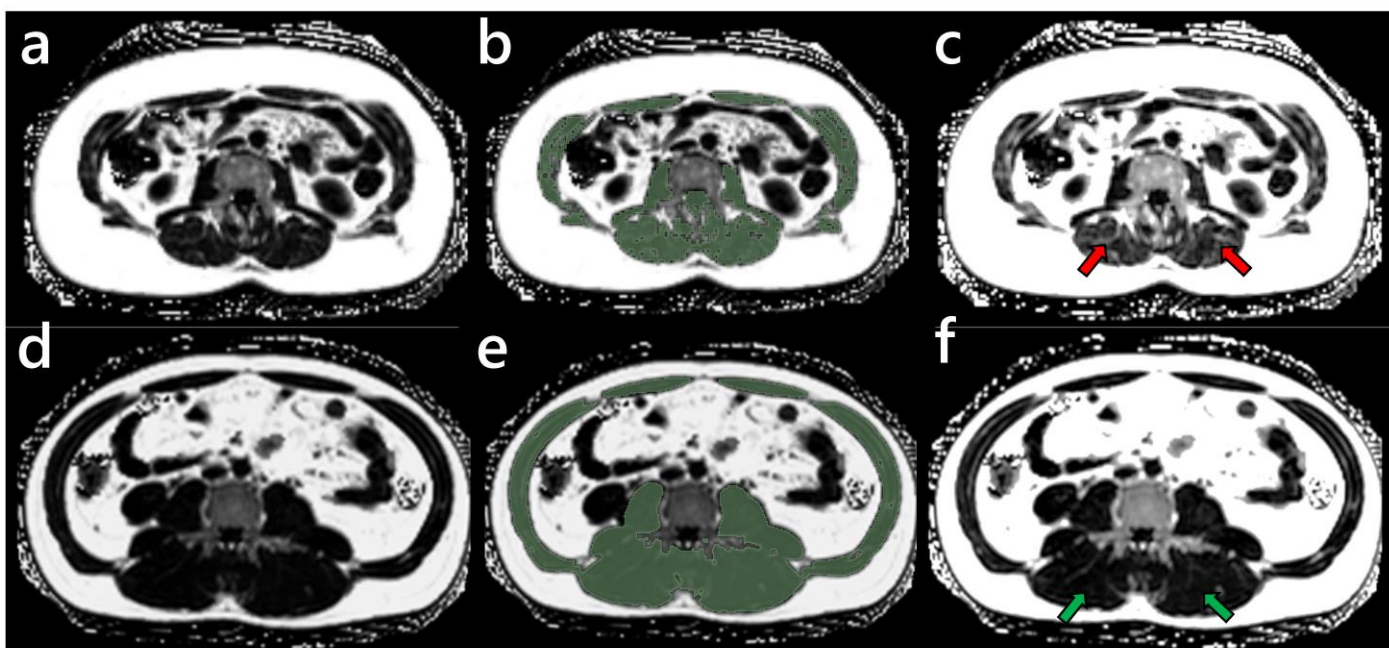
Incident cases of type-2 diabetes ($n = 146$) are within and outside of the randomly selected subcohort.

The case-cohort study in Japan comprised 754 participants of whom 658 were in the randomly selected subcohort. There were 146 incident cases of type-2 diabetes, including 50 “overlap” cases.

Analysis 1 was conducted using data from the randomly selected subcohort (Japan, $n = 658$).

Analysis 2 and analysis 3 were conducted using data from all participants in the case-cohort study (Japan, $n = 754$).

Analysis 4 was conducted using data from the cohort in Germany ($n = 319$)

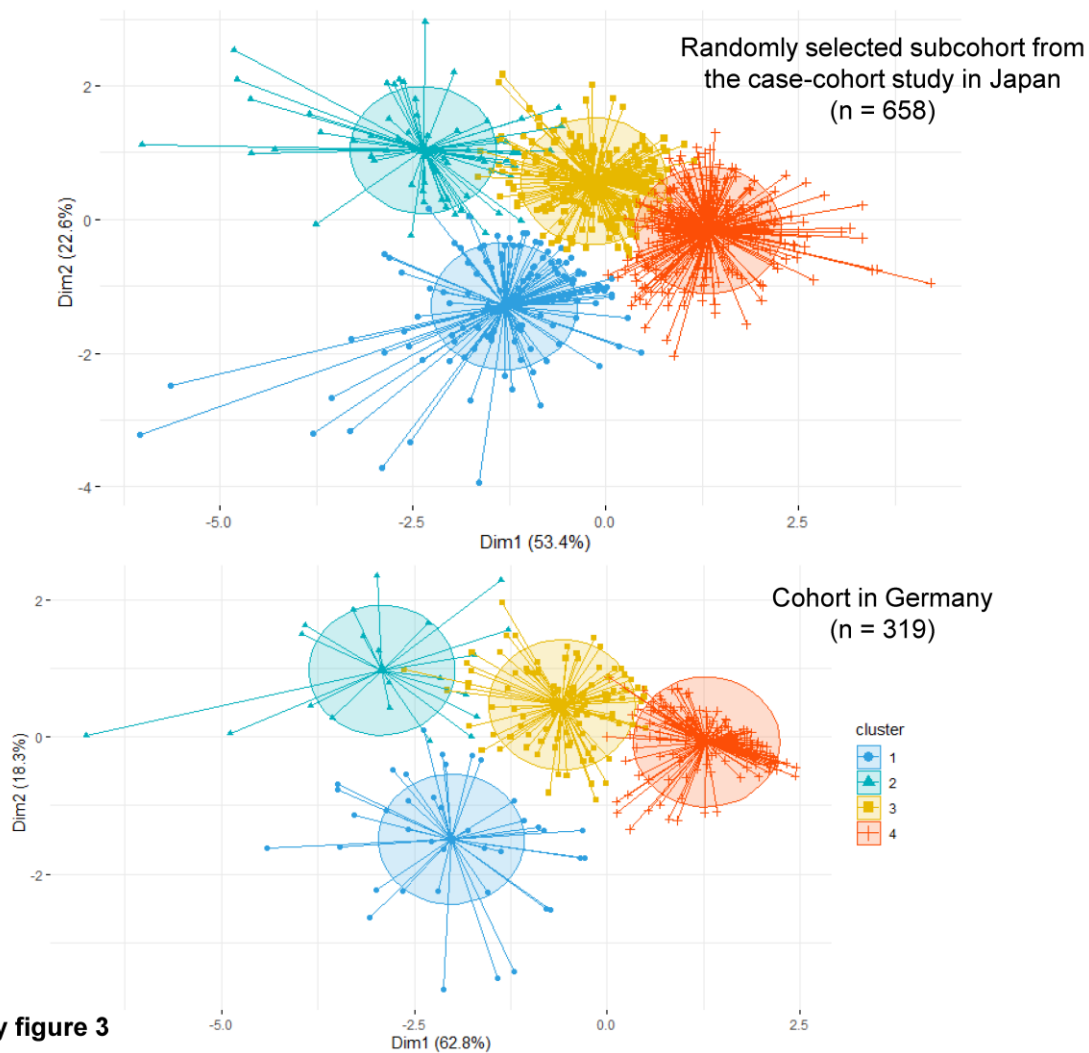


Supplementary figure 2

Supplementary Figure 2. Axial PDFF images at the level of the L3 lumbar segment.

PDFF images from a 50-year-old woman (a-c) and a 34-year-old man (d-f) show the muscle area in green (b and e) and muscle fat (c and f) resulting in a mean of 11.7% in the woman and 4.8% in the man.

PDFF, proton density fat fraction



Supplementary figure 3

Supplementary Figure 3. Cluster plots

Four clusters based on k-means clustering are shown in each of the two cluster plots. Principal components analysis was conducted to project data onto the first two principal components. Data variation (%) of the first principal component (Dim1) and the second principal component (Dim2) are shown on the axes.

Cluster 1: Hepatic steatosis, Cluster 2: Pancreatic steatosis, Cluster 3: Trunk myosteatosi s , Cluster 4:

Steatopenia

	Cluster 1 Hepatic steatosis	Cluster 2 Pancreatic steatosis	Cluster 3 Trunk myosteatosi	Cluster 4 Steatopenia
Diabetes risk	↑ ↑	↑ ↑	↑	Reference
Insulin sensitivity	↓↓↓	↓↓	↓	Reference
Insulin secretion adjusted for insulin sensitivity	→	↓	↓	Reference

Supplementary figure 4

Supplementary Figure 4. Summary of metabolic characteristics in fat distribution clusters